

# Non-Markovian relaxation in an open quantum system

## Polynomial approach to the solution of the quantum master equation

T. Mančal<sup>a</sup> and V. May

Institut für Physik der Humboldt-Universität zu Berlin, Hausvogteiplatz 5-7, 10117 Berlin, Germany

Received 12 April 2000 and Received in final form 2 September 2000

**Abstract.** Non-Markovian dynamics in open quantum systems is characterized by a time–non-locality in the equation of motion valid for the reduced density operator. An expansion of this density matrix equation with respect to Laguerre polynomials is used to tackle the time–non-locality. The applicability and the numerical limitations of the method are discussed in detail. In order to illuminate the characteristics of non-Markovian dynamics the reference example is studied of a single quantum degree of freedom moving in a harmonic potential and being embedded in a heat bath. If interpreted as the photoinduced dynamics of nuclear motion in polyatomic molecules we can suggest two clear signatures of non-Markovian dynamics observable in ultrafast optical experiments, firstly a pronounced and somewhat irregular oscillatory behavior of the vibrational level populations, and secondly a separation of the vibrational wavepacket into a double-structure.

**PACS.** 31.70.Hq Time-dependent phenomena: excitation and relaxation processes, and reaction rates – 82.70.Dd Colloids – 02.60.Cb Numerical simulation; solution of equations – 02.60.Nm Integral and integrodifferential equations

## 1 Introduction

If a small subsystem embedded in a large environment is studied it is a common observation that the subsystem dynamics shows retardation effects. These retardation effects are caused by the coupling to the environmental degrees of freedom and can be accounted for by certain environmental correlation functions. For the time-evolution of a probability distribution, the type of equations showing retardation effects are known as non-Markovian equations of motion. The neglect of the retardation is usually termed Markov approximation (see, for example [1,2]).

Although typical for quantum as well as classical systems we will concentrate the following in non-Markovian effects taking place in a small quantum system (active systems S) interacting with a macroscopic heat bath (reservoir R). For such a case the complete system S + R has to be described by the time-dependent quantum statistical operator  $\hat{W}(t)$ . The appropriate quantity to follow the dynamics of S is given by the reduced statistical operator  $\hat{\rho}(t)$ . It is obtained from  $\hat{W}(t)$  by taking the trace with respect to the reservoir states, *i.e.*  $\hat{\rho}(t) = \text{tr}_R\{\hat{W}(t)\}$ . Since the equation of motion determining  $\hat{\rho}(t)$  is of the operator type, retardation and thus non-Markovian behavior is governed by a time non-local superoperator acting on  $\hat{\rho}$  according to  $\int_0^t d\tau \mathcal{M}(\tau)\hat{\rho}(t - \tau)$ . The quantity  $\mathcal{M}$

defines the (superoperator) memory kernel. According to the well-established approach leading to the Nakajima-Zwanzig equation for  $\hat{\rho}(t)$  an exact expression for  $\mathcal{M}(\tau)$  is known (see, *e.g.* [1,3]), which usually serves as a starting point for perturbational expansions. The decay of  $\mathcal{M}(\tau)$  with increasing  $\tau$  fixes the characteristic time-scale  $\tau_{\text{mem}}$  for which retardation (memory) effects are important. It is worth mentioning here that the path integral representation of the reduced density matrix incorporates retardation effects also (for a recent overview we mention [4]).

As an alternative to the Nakajima-Zwanzig equation an equation of motion for  $\hat{\rho}(t)$  has been suggested which is exact but local in time, *i.e.* dissipation is described by  $\mathcal{D}(t)\hat{\rho}(t)$ . This results in the so-called time-convolutionless density matrix equation [5] (see also the discussion in [6]). Within this approach the absence of the time-nonlocality has been achieved by introducing into  $\mathcal{D}(t)$  the reverse time-evolution from the actual time back to the initial time. This can be understood as the presence of additional partial expansions with respect to the perturbation (the system-reservoir coupling). Both density matrix equations may be related to one another if one expands  $\hat{\rho}(t - \tau)$ , which appears in the time-nonlocal approach, in powers of  $\tau$  [7]. If the second-order version of  $\mathcal{D}(t)$  (with respect to the system-reservoir coupling) is taken a nearly correct reproduction of the non-Markovian dynamics (of this second-order perturbation type) can be obtained [8].

<sup>a</sup> e-mail: mancal@physik.hu-berlin.de

The discussion of the various problems related to non-Markovian dynamics in open quantum systems has received a lot of interest in recent years [6,7,9–17]. This has been mainly initiated by the developments in femtosecond spectroscopy. It is typical for this type of laser spectroscopy that one can achieve pulse lengths (in the optical and near infrared region) smaller than the characteristic time  $\tau_{\text{mem}}$  of the retarded system-environment interaction. If electron and even vibrational dynamics in molecular or solid state systems is considered the time-scale of this motion may also match  $\tau_{\text{mem}}$ . This fact underlines the well-accepted opinion that a proper description of systems in the condensed phase interacting with ultra-short laser pulses with duration in the region of some 10 fs desires a non-Markovian description of dissipation. For higher intensities of the laser pulse, one additionally has to incorporate the pulse modulation of the system-environment coupling (laser intensity dependence of dissipation) [16,17].

A direct solution of the non-Markovian density operator equation requires the necessity to carry out an integration back into the past including the density operator. In particular, for memory kernels with a comparable large  $\tau_{\text{mem}}$  this would become a cumbersome attempt. There exist different alternative approaches to circumvent this difficulty. To account for the time-nonlocality in simple few level systems the density matrix theory can be combined with the Laplace transformation method [9–11]. Additionally, this approach allows to relate the effect of dissipation described in the time-domain to the frequency-domain. For example, non-Markovian dynamics is related to the frequency dependence of absorption line-broadening (see also [7,18]). To determine the memory kernel of larger systems one makes the assumption that the spectral density of the environmental modes can be represented by a Lorentzian type of distribution. The resulting exponential form of the memory kernel offers the possibility to use a simple predictor-corrector method for the integration of the equation of motion [13,16]. The replacement of the time-nonlocality by adding to an existing system some fictitious modes has been suggested in [19]. The additional modes can be treated within a Markov approximation and have to be chosen in such a manner that they reproduce the spectral density of the environment. Clearly, if one needs too many fictitious modes to approximate the spectral density the approach becomes inefficient.

In the present work we explain an alternative and quite general method which enables us to treat the non-Markovian density matrix equation in an exact manner and for any type of spectral density. The approach is based on an expansion with respect to certain special functions [20,21], which results in a conversion of the integro-differential equations into algebraic ones. From previous work in references [22,23] it follows that the most suitable type of special functions is given by the orthonormal set of Laguerre polynomials defined as

$$L_n(t) = \frac{1}{n!} e^t \left( \frac{d}{dt} \right)^n (t^n e^{-t}). \quad (1)$$

Beside different other properties given below, Laguerre polynomials obey the following important equation

$$\int_0^t d\tau L_n(t-\tau)L_m(\tau) = L_{n+m}(t) - L_{n+m+1}(t). \quad (2)$$

This represents the key relation to handle any type of time non-locality. If all ingredients of the non-Markovian density matrix equation are expanded with respect to the Laguerre polynomials the difficulty to treat the retardation effects has been overcome.

Such a relative simple replacement of the time non-locality enables us to describe the non-Markovian dynamics of multi-level quantum systems. The efficiency of the Laguerre polynomial expansion method and the stability and accuracy of the related numerics will be of special interest in this connection. All these questions are discussed in Section 4. But before doing this we specify in the following section our system S as well as the coupling to the environment and introduce the respective Hamiltonian. Furthermore, we offer the non-Markovian and the Markovian version of the density matrix equation to be solved (quantum master equation, QME). The Laguerre polynomial method will be presented in Section 3. All numerical results underlying the characteristics of non-Markovian quantum dynamics can be found in Section 4. Some details of the method are discussed in the appendix together with a simple reference example for which the non-Markovian dynamics can be described analytically.

## 2 The non-Markovian quantum master equation

In line with the separation of the whole system S + R into the (active) system and the reservoir part, the complete Hamiltonian is written as  $H = H_S + H_{S-R} + H_R$ , involving the system Hamiltonian  $H_S$ , the reservoir Hamiltonian  $H_R$  and the coupling Hamiltonian  $H_{S-R}$  between both. According to the purposes of the present paper we chose a simple example for  $H$ , namely a harmonic oscillator coupled to a macroscopic reservoir of thermalized harmonic oscillators. Introducing a notation with a dimensionless coordinate  $Q = b + b^+$  related to the oscillator annihilation and creation operator, the system Hamiltonian simply reads  $H_S = T + U \equiv \hbar\omega_{\text{vib}}b^+b$  with oscillator potential  $U(Q) = \hbar\omega_{\text{vib}}Q/4$ . (Although quite simple, the oscillator serves as a minimal model to describe, *e.g.* vibrational dynamics in a given electronic level of a molecular system.)

The system-bath interaction is taken in the following form

$$H_{S-R} = K(Q)\Phi(Z), \quad (3)$$

where the operator  $K(Q)$  operates exclusively in the Hilbert space of the active system states, while  $\Phi(Z)$  is defined in the space of the reservoir states and depends on the reservoir coordinates.  $H_R$  corresponds to the Hamiltonian of the large number of reservoir harmonic oscillators. In order to simulate a simple system-reservoir coupling

we will take the bilinear *ansatz*, where  $K(Q) = Q$ . Furthermore, we suppose  $\hat{\Phi}(Z) = \hbar \sum_{\xi} k_{\xi} Z_{\xi}$ , with  $k_{\xi}$  being the respective coupling constant.

There are various physical realizations of a quantum oscillator embedded in a thermal environment. Concentrating here on femtosecond spectroscopy of molecular systems we will identify the oscillator by a vibrational degree of freedom of a molecule which undergoes electronic transitions after photoexcitation (see, *e.g.* [3]). Mostly, the oscillator equilibrium position changes upon the electronic transition resulting in an electron-vibrational coupling. If the electronic transition is realized by a light-pulse which is comparable to or shorter than the vibrational oscillation period the coordinate is prepared in a nonequilibrium state and respective wavepacket dynamics follows. The *active* coordinate is coupled to other vibrational degrees of freedom. If their equilibrium position changes only slightly in the course of electronic transitions they can be described as a thermal reservoir of passive coordinates. In cases where a normal-mode analysis can be carried out it is natural to describe the passive vibrational coordinates by a (large) set of independent harmonic oscillators.

The dissipative dynamics of the simple system introduced so far is described by the statistical operator  $\hat{\rho}(t)$  reduced to the state space of the active system oscillator. Carrying out a second-order perturbation expansion with respect to the system-bath interaction we end up with the QME (see, *e.g.* [3])

$$\frac{\partial}{\partial t} \hat{\rho}(t) = \hat{I}(t; \hat{W}(t_0)) - i\mathcal{L}_S \hat{\rho}(t) - \hat{D}(t, t_0; \hat{\rho}). \quad (4)$$

The first term on the right-hand side describes correlations caused by an initial state of the whole system S + R which does not factorize into a pure system part and a pure reservoir part. It is usually assumed that such initial correlations decay on a time-scale of  $\tau_{\text{mem}}$ . Therefore, we will neglect  $\hat{I}$ . (A numerical confirmation of this fast decay of  $\hat{I}$  can be found in [16]. But also compare the reasoning given at the beginning of Section 4 for excited-state preparation by external fields.) The reversible part of the dynamics are governed by the Liouvillian  $\mathcal{L}_S \equiv [H_S, \dots]_- / \hbar$ . And, the part of equation (4) given by  $\hat{D}$  describes dissipation and includes the convolution of the memory kernel superoperator  $\mathcal{M}$  and the density operator

$$\hat{D}(t, t_0; \hat{\rho}) = \int_0^{t-t_0} d\tau \mathcal{M}(\tau) \hat{\rho}(t - \tau). \quad (5)$$

(The relation given in the introductory part follows for the initial time  $t_0 = 0$ .) According to the second-order perturbation theory (inherent to the QME) the memory kernel superoperator reads in detail [3, 24]

$$\begin{aligned} \mathcal{M}(\tau) \hat{\rho}(t - \tau) = & \\ & \left( C(\tau) [K(Q), U_S(\tau) K(Q) \hat{\rho}(t - \tau) U_S^\dagger(\tau)]_- \right. \\ & \left. - C^*(\tau) [K(Q), U_S(\tau) \hat{\rho}(t - \tau) K(Q) U_S^\dagger(\tau)]_- \right). \quad (6) \end{aligned}$$

The expression contains the reservoir correlation function which is given as

$$C(t) = \frac{1}{\hbar^2} \text{tr}_R \{ \hat{R}_{\text{eq}} U_R^\dagger(t) \hat{\Phi} U_R(t) \hat{\Phi} \}. \quad (7)$$

Here, we introduce  $\hat{R}_{\text{eq}} = \exp -H_R/k_B T / \text{tr}_R \{ \exp -H_R/k_B T \}$ . The time-evolution operators used in the two foregoing equations are defined as  $U_A(t) = \exp -iH_A t / \hbar$  with  $A = S, R$ . The definition of  $C(t)$  takes into consideration that  $\text{tr}_R \{ \hat{R}_{\text{eq}} \hat{\Phi} \} = 0$ . As it is well known (see, *e.g.* [3]) the correlation function can be expressed as

$$C(t) = \int d\omega e^{-i\omega t} (1 + n(\omega)) (J(\omega) - J(-\omega)), \quad (8)$$

with  $n(\omega) = 1/(\exp(\hbar\omega/k_B T) - 1)$  being the Bose-Einstein distribution.  $J(\omega)$  represents the spectral density of reservoir oscillators

$$J(\omega) = \sum_{\xi} k_{\xi}^2 \delta(\omega - \omega_{\xi}) = \Theta(\omega) J_0 j(\omega), \quad (9)$$

where the function  $j(\omega)$  has been normalized to 1 in the frequency interval between 0 and  $\infty$ . ( $\Theta(\omega)$  denotes the unit-step function.) For the computations explained below we use the *ansatz*

$$j(\omega) = \frac{\omega}{\omega_c^2} e^{-\omega/\omega_c}. \quad (10)$$

The inverse of the cut-off frequency  $\omega_c$  gives a rough measure for the characteristic time  $\tau_{\text{mem}}$  on which the correlations of the reservoir degrees of freedom decay. We will denote the inverse of  $\omega_c$  by  $t_c$ .

For the following considerations it is most appropriate to change to the state (energy) representation of the QME. To this end equation (4) is expanded with respect to the *eigenstates*  $|a\rangle, |b\rangle$  etc., of  $H_S$ . In the course of the numerical calculations we have to identify these states with the harmonic oscillator *eigenfunctions*  $|M\rangle$ . The resulting state representation of the QME reads [3]

$$\frac{\partial}{\partial t} \rho_{ab}(t) = -i\omega_{ab} \rho_{ab}(t) - \sum_{c,d} \int_0^t d\tau \mathcal{M}_{ab,cd}(\tau) \rho_{cd}(t - \tau). \quad (11)$$

Note the special choice  $t_0 = 0$ , and the abbreviation  $\omega_{ab} = (E_a - E_b)/\hbar$ , where the  $E_a$  are *eigenvalues* of  $H_S$ . The tetradic matrix  $\mathcal{M}_{ab,cd}(\tau)$  following from the memory kernel superoperator reads in detail

$$\begin{aligned} \mathcal{M}_{ab,cd}(\tau) = & \\ & \delta_{a,c} \sum_e M_{de,eb}(-\tau) e^{i\omega_{ea}\tau} + \delta_{b,d} \sum_e M_{ae,ec}(\tau) e^{i\omega_{be}\tau} \\ & - M_{db,ac}(-\tau) e^{i\omega_{bc}\tau} - M_{db,ac}(\tau) e^{i\omega_{da}\tau}, \quad (12) \end{aligned}$$

with

$$M_{ab,cd}(\tau) = C(\tau) \langle a|K|b\rangle \langle c|K|d\rangle. \quad (13)$$

If the memory function dies out fast the dissipative part of equation (11) is usually simplified in carrying out the Markov approximation. Therefore, one changes from  $t - \tau$  to  $t$  in the argument of the density operator. The latter procedure has to be done in the interaction representation by taking  $\rho_{ab}(t - \tau) \approx \exp(i\omega_{ab}\tau)\rho_{ab}(t)$ . As an additional approximation one can prolongate the upper bound of the integral to infinity. It yields the dissipative part of equation (11) as  $\sum_{cd} \mathcal{R}_{ab,cd}\rho_{cd}$  where the complex Redfield tensor reads

$$\mathcal{R}_{ab,cd} = \delta_{a,c} \sum_e \hat{M}_{be,ed}^*(-\omega_{ed}) + \delta_{b,d} \sum_e \hat{M}_{ae,ec}(\omega_{ce}) - \hat{M}_{ca,bd}^*(-\omega_{bd}) - \hat{M}_{db,ac}(\omega_{ca}). \quad (14)$$

Here,  $\hat{M}_{ab,cd}(\omega)$  denotes the half-sided Fourier transform of the function introduced in equation (13) (note  $\hat{M}_{ab,cd}(\omega) = \hat{M}_{cd,ba}^*(-\omega)$ ). The usual Redfield tensor is obtained as the real part of the above given expression [3, 24, 25]. This QME is local in time, so the solution can be found by a standard Runge-Kutta type method [26].

### 3 Solution of the non-Markovian equation of motion

The equations of motion (11) represent a set of coupled integro-differential equations. As already claimed an expansion of equation (11) with respect to Laguerre polynomials will remove the time nonlocality as well as the time derivative and leads to a set of algebraic equations. In solving these equations one obtains the expansion coefficients of the density matrix from the expansion coefficients of the memory kernel which have to be computed separately. This computation will be presented in such a general form that any restriction to a special type of the memory kernel (or the reservoir correlation function) can be avoided.

#### 3.1 Laguerre polynomial expansion

The key property of the Laguerre polynomials which enable an effective application of the method is their orthogonality with respect to the scalar product

$$(f, g) = \int_0^\infty d\theta e^{-\theta} f(\theta)g(\theta). \quad (15)$$

In our application to the solution of the equation of motion, *i.e.* the determination of the time evolution of the density matrix, the dimensionless variable  $\theta$  has to be properly mapped on the time  $t$ . This can be done *via* a relation

$$\theta = \frac{t}{t_{\text{char}}}, \quad (16)$$

where the time-constant  $t_{\text{char}}$  roughly fixes the characteristic time-interval in which the function to be expanded by Laguerre polynomials can be properly described.

Using now the dimensionless time  $\theta$ , the expansion of the various parts of equation (11) is achieved according to

$$\rho_{ab}(\theta t_{\text{char}}) = \sum_{n=0}^{\infty} \rho_{ab}^{(n)} L_n(\theta), \quad (17)$$

and

$$\mathcal{M}_{ab,cd}(\theta t_{\text{char}}) = \sum_{n=0}^{\infty} \mathcal{M}_{ab,cd}^{(n)} L_n(\theta). \quad (18)$$

Applying now the scalar product (15) we obtain, for example, the expansion coefficients of the density matrix defined as

$$\rho_{ab}^{(n)} = \int_0^\infty d\theta e^{-\theta} L_n(\theta) \rho_{ab}(\theta t_{\text{char}}). \quad (19)$$

The initial values of the density matrix can be related to the complete sum of the expansion coefficients according to (note  $L_n(\theta = 0) = 1$ )

$$\rho_{ab}(t = 0) = \sum_{n=0}^{\infty} \rho_{ab}^{(n)}. \quad (20)$$

Beside the fundamental property, equation (2) we take into account [23, 27, 28]

$$\frac{\partial}{\partial \theta} L_n(\theta) = - \sum_{m=0}^{n-1} L_m(\theta) \quad (21)$$

and carry out Laguerre polynomial expansion of the non-Markovian QME, equation (11). It follows a recurrence formula for the density matrix expansion coefficients

$$\sum_{cd} \left( (i t_{\text{char}} \omega_{ab} + 1) \delta_{ac} \delta_{bd} + t_{\text{char}}^2 \mathcal{M}_{ab,cd}^{(0)} \right) \rho_{cd}^{(n)} = \rho_{ab}(t = 0) - \sum_{m=0}^{n-1} \left( \rho_{ab}^{(m)} + t_{\text{char}}^2 \sum_{cd} \left[ \mathcal{M}_{ab,cd}^{(n-m)} - \mathcal{M}_{ab,cd}^{(n-m-1)} \right] \rho_{cd}^{(m)} \right). \quad (22)$$

Such an existence of a recurrence formula represents the great advantage of the Laguerre polynomial method compared to the Laplace transformation technique. To get within the latter method, the transformed density matrix, one has to invert the complete Laplace-transformed tetradic coefficient matrix. However, this can be avoided here. Finally, to compute the expansion coefficients of the density matrix it remains to determine the expansion coefficients of the memory kernel.

#### 3.2 Determination of the memory kernel expansion coefficients

The memory kernel expansion coefficients  $\mathcal{M}_{ab,cd}^{(n)}$  have to be computed in similarity to equation (19). Unlike to [23]

it is not possible to obtain these coefficients analytically. Since we expect the need of using (at least) some hundreds of polynomials it becomes necessary to evaluate the respective time integrals with polynomials of high order. To do this by an ordinary numerical method would be either inaccurate or inconveniently time consuming. Therefore, we try to proceed analytically as far as possible.

A detailed inspection of relation (12) demonstrates that we have to handle contributions of the type ( $\Delta\tilde{\omega} = t_{\text{char}}\Delta\omega$  where  $\Delta\omega$  denotes one of the various transition frequencies)

$$\tilde{C}^{(n)} = \int_0^\infty d\theta L_n(\theta) e^{i\Delta\tilde{\omega}\theta} e^{-\theta} C(\pm\theta t_{\text{char}}). \quad (23)$$

This expression enables us to fix the value of  $t_{\text{char}}$ . Since we will consider correlation functions decaying on a time-scale of some 10 fs we set  $t_{\text{char}} = 10$  fs. Indeed, such a value is large enough to avoid any suppression of  $C(t)$  by the exponential prefactor.

To calculate the above type of integrals we proceed as follows. First we note that  $C(t)$  follows from an inverse Fourier transformation according to equation (8). In the general case this Fourier transformation has to be carried out numerically, and, consequently, the values of the function  $C(t)$  are given for a set of points  $t_0, t_1, \dots, t_N$  on the time axes, corresponding to  $\theta_0, \theta_1, \dots, \theta_N$  in dimensionless time. Such a set can be interpolated by the so-called cubic splines [26], which result in a function, analytical by-parts and continuous up to the second derivative. Then, between any two points  $\theta_j, \theta_{j+1}$  of the set, the function  $C(\theta t_{\text{char}})$  is represented by a cubic polynomial and the integral (23) turns to a sum of the integrals

$$\tilde{C}_{\text{spl}}^{(n,j)} = \int_{\theta_j}^{\theta_{j+1}} d\theta L_n(\theta) e^{i\Delta\tilde{\omega}\theta} e^{-\theta} C_{\text{spl}}^{(j)}(\pm\theta t_{\text{char}}), \quad (24)$$

with  $C_{\text{spl}}^{(j)}(t)$  being a spline interpolation of  $C(\pm t)$  in the interval  $[t_j, t_{j+1}]$ . For all of these integrals a special recurrence formula can be derived, and it becomes possible to evaluate the integrals for any polynomial order and any value of  $\Delta\omega$ . For more details see Appendix A.

With this technique we can evaluate the expansion coefficients  $\mathcal{M}_{ab,cd}^{(n)}$  with sufficient accuracy and a smaller computation time. The accuracy of the above given scheme can be easily checked by a comparison of the original memory function, equation (18) and its numerically obtained approximation. Having the expansion coefficients  $\mathcal{M}_{ab,cd}^{(n)}$  at hand, we get the expansion coefficients  $\rho_{ab}^{(n)}$  by a straightforward solution of the algebraic equations (22).

## 4 Results

If the Laguerre polynomial expansion is to be applied, initially one has to gain some insight into the convergence

behavior, the numerical stability and the accuracy. This will be done in the following together with the investigation of the non-Markovian dynamics of the chosen model system.

To have a concrete physical system in mind we take the parameters according to the previously studied minimal model of a polyatomic molecule in solution (see [17,29]). Therefore, the oscillator studied here has to be understood as corresponding to an effective molecular vibrational degree of freedom moving in a certain potential energy surface and having a quantum energy of 190 meV. According to this value the correlation function  $C(t)$  taken for room temperature does not differ substantially from  $C(t)$  at zero temperature for which the actual calculations have been carried out. The initial condition for our QME has been chosen in the form of the displaced oscillator ground state wave function. Such an initial state may be achieved via an electronic transition ending up in the potential energy surface under discussion. It corresponds to an excited electronic state and has been populated *via* the action of an ultrafast laser pulse. As explained in detail [8], such an external field preparation of an excited electronic state removes the need to account for initial correlations present in the basic QME (4). Therefore, the solution of the QME becomes valid already at an earlier time region.

For the density matrix we may set (note the use of the oscillator quantum numbers instead of  $a, b$  etc.)

$$\rho_{MN}(t=0) = \langle M | D^+(g) | 0 \rangle \langle 0 | D(g) | N \rangle \quad (25)$$

where the displacement operator  $D^+(g) = \exp g(b - b^\dagger)$  has been introduced. Since the wavepacket has been put between the third and fourth excited vibronic level the dimensionless displacement  $g$  amounts to the value 2. The QME is solved for inverse cut-off frequencies  $t_c$  of the spectral density, equation (9) between 10 and 100 fs.

### 4.1 Applicability and accuracy of the polynomial method

It has been already highlighted in [23] and can be made obvious by an inspection of equation (22) that the accuracy of the memory kernel expansion determines the accuracy of the computed density matrix elements. Having at hand a sufficient good approximation of the memory kernel for the time interval  $[t_1, t_2]$  one may expect that the density matrix expansion results in the same accuracy.

A convenient proof of the convergence of the expansion is to compute the contribution given by a few last terms in the expansion while enlarging the number of expansion coefficients. However, in a case where the function  $f(t)$  to be expanded is known we can easily check the accuracy of the actual expansion  $f_{\text{exp}}(t; N) = f_{\text{exp}}(\theta t_{\text{char}}; N) = \sum_{n=0}^N f^{(n)} L_n(\theta)$  of order  $N$  by introducing

$$\sigma(t_1, t_2; N) = \frac{1}{t_2 - t_1} \int_{t_1}^{t_2} dt |f(t) - f_{\text{exp}}(t; N)|. \quad (26)$$

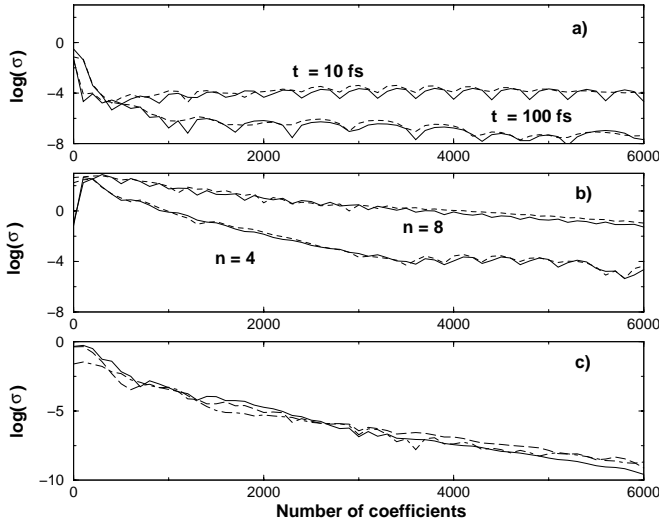


**Fig. 1.** Accuracy of the Laguerre polynomial expansion. The measure  $\sigma(t_a = 0, t_b = 300 \text{ fs}; N)$ , equation (26) and  $\Delta\sigma(t_a = 0, t_b = 300 \text{ fs}; N + 100, N)$ , equation (27) are drawn *versus* the expansion order  $N$ . Part (a)  $\sigma$  (solid line) and  $\Delta\sigma$  (dashed line) for correlation function  $C(t)$  with different  $t_c$ . Part (b) The same as in part (a) but for the function  $C(t)e^{i\omega_{\text{vib}}t}$  the single value  $t_c = 10 \text{ fs}$  but for different  $\Delta N$ . Part (c)  $\Delta\sigma(t_a = 0, t_b = 300 \text{ fs}; N + 100, N)$  *versus*  $N$  for the diagonal elements of the harmonic oscillator density matrix. Solid line:  $\rho_{00}$ , dashed line:  $\rho_{44}$ , dashed-dotted line:  $\rho_{88}$ .

The expression gives the absolute value of the difference between the original function and its  $N$ 'th order expansion averaged with respect to the time interval  $[t_1, t_2]$ . If the function  $f(t)$  is not known one has to compare different orders  $N$  of the expansion, say  $N$  and  $N + \Delta N$ , ( $\Delta N > 0$ ). For this reason one may introduce as a measure of accuracy

$$\Delta\sigma(t_1, t_2; N + \Delta N, N) = \frac{t_{\text{char}}}{t_2 - t_1} \times \int_{t_1/t_{\text{char}}}^{t_2/t_{\text{char}}} d\theta \left| \sum_{n=N+1}^{N+\Delta N} f^{(n)} L_n(\theta) \right|. \quad (27)$$

In Figure 1 we demonstrate the accuracy of the polynomial expansions of the correlation function and the density matrix elements. The quantities  $\sigma(0, 300 \text{ fs}; N)$ , equation (26) as well as  $\Delta\sigma(1, 300 \text{ fs}; N + 100, N)$ , equation (27) are presented in part (a) of Figure 1 as a function of the order  $N$  of the Laguerre polynomial expansion. Both measures,  $\sigma$  and  $\Delta\sigma$  have been calculated for the case of the correlation function  $C(t)$ , equation (8) with inverse cut-off frequencies  $1/\omega_c = t_c = 10 \text{ fs}$  and  $100 \text{ fs}$ . In part (b) of Figure 1 the same quantities are drawn for  $C(t)e^{i\omega t}$  with  $n = 4, 8$  and with  $t_c = 10 \text{ fs}$ .

Both measures show a strong decay for  $N$  less than  $10^3$ . Afterwards a saturation appears if  $N$  is further increased. As it has to be expected the correlation function with  $t_c = 100 \text{ fs}$  needs a higher expansion order to reach saturation. The saturation behavior points out the fact that

the accuracy of the expansion reaches its limit if it coincides with the accuracy of the spline approximation. Of course, this can be improved by shortening the step length of the spline approximation. Interestingly,  $\sigma$  as well as  $\Delta\sigma$  are of the same order, this indicates that they can be used alternatively.

Next, the accuracy of the density matrix expansion is estimated where the only measure to be used is given by  $\Delta\sigma$ , equation (27). The accuracy of this expansion is determined by that of the memory kernel. But different components of the correlation function are expanded with different accuracies. For example, some highly oscillating terms do not substantially contribute to the dynamics, and an expansion with low accuracy seem to be sufficient.  $\Delta\sigma(0, 300 \text{ fs}; N + \Delta N, N)$  as a function of  $N$  for  $\Delta N = 100$  and resulting from the expansion of different density matrix elements is presented in part (c) of Figure 1.

## 4.2 Numerical results for the model system

Based on the technical details which have to be noticed if the Laguerre polynomial expansion is used, we proceed in studying the non-Markovian dynamics of our model system. Of basic interest would be a comparison with the dynamic behavior present in the limit of the Markov approximation. This comparison can be carried out in different ways. First we can try to compare those different types of non-Markovian dynamics which obey the same Markov-limit as a common feature. In comparing equation (12) with equation (14) we see that the demand for the same Markov-approximation is equivalent with the demand for the same Redfield tensor. This can be translated to the demand that the different types of correlation function  $C(t)$  used in the comparison should have the same values  $C(\omega)$  at certain frequencies. In the present case of a harmonic oscillator there remains only the single value  $C(\omega_{\text{vib}})$  of  $C(\omega)$  where all correlation functions should coincide.

An alternative scheme to compare different types of non-Markovian dynamics could be based on the application of different correlation functions  $C(t)$  with different extensions along the time-axis, but with the same integral value. However, we found the first of these approaches to be more suitable for our purpose. In the Markov-limit and in so-called secular approximation (see, *e.g.* [3]) the quantity  $C(\omega_{\text{vib}})$ , and in the present  $T = 0$ -limit  $J(\omega_{\text{vib}})$ , can be directly related to the inverse life-time of an oscillator level, *i.e.* we have  $1/\tau_M = 2\pi M J(\omega_{\text{vib}})$ . Thus, to compare non-Markovian results with different correlation functions we choose the coupling in such a way, that corresponds in the Markov-limit to the same life-time of the first excited oscillator level.

To study different dynamic regimes of the model system we first consider in which manner the coupling-strength of the system oscillator to the reservoir ( $j_0$  in our case, see Eq. (9)) influences the dynamics. It is a well-accepted fact that the positivity of the density matrix can be violated if the coupling strength is enlarged beyond a critical value (see, *e.g.* [12]). This drawback also has to be expected for the non-Markovian QME. But decreasing

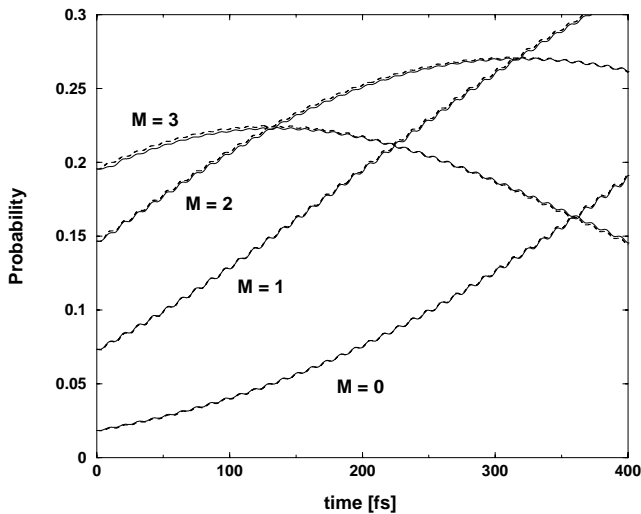


**Fig. 2.** Occupation probabilities of the first four oscillator levels. The solution of the non-Markovian QME (full lines) is compared with the solution applying the Markov approximation (dashed lines). Used parameters:  $t_c = 10$  fs,  $J(\omega_{\text{vib}}) = 3.5 \times 10^{-4}$ /fs (corresponding to the life-time  $\tau_1 \approx 450$  fs).

the decay-time of  $C(t)$  one may reach the limit  $C(t) \sim \delta(t)$  resulting in the Lindblad-form of dissipation [3]. Therefore, we have to expect that our simulations may show the violation of the positivity of the density matrix if the coupling to the reservoir is increased. However, this defect of the theory should be less dominant if the decay time of  $C(t)$  is shortened further and further.

Let us study the influence of the time-constant  $t_c$  which determines the time-scale the memory kernel decays within the area of the valid coupling strengths. Figure 2 illustrates the case of a short memory for which  $t_c$  amounts about half of the oscillator period. Drawn are the oscillator level populations  $P_M(t) = \rho_{MM}(t)$  versus time with an initial distribution according to equation (25). As expected the Markov and non-Markov results are almost identical within the studied time interval.

The case where the correlation time  $t_c$  is comparable to the period of the oscillator motion is shown in Figure 3. Even for this case the overall character of the time development of the probabilities is very similar. However, one can notice a different behavior for the Markov-case and the non-Markov approach shortly after the time evolution starts. But at  $t > t_c$  both types of solutions follow similar patterns. This has also been reported by other authors [12,30] and resulted in the proposal of the artificial slippage of initial conditions in order to reproduce the solution of the non-Markovian QME using Markovian equations after a certain initial time interval is exceeded. (Note also the slight difference between the Markov case of Fig. 2 and of Fig. 3 which is originated by the presence of an imaginary part in Eq. (14).)

Calculations similar to those already discussed have been also done for much larger  $t_c$ . In this case and for acceptable coupling strength to the reservoir we could not observe a substantial deviation (up to the time region of

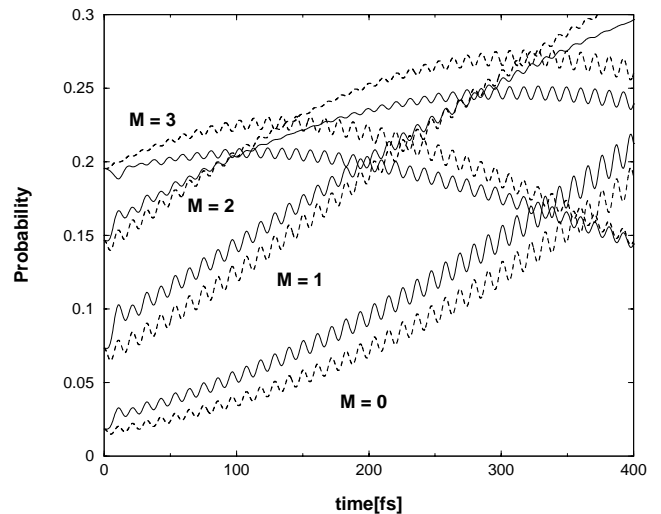


**Fig. 3.** Occupation probabilities of the first three oscillator levels. The solution of the non-Markovian QME (full lines) is compared with the solution applying the Markov approximation (dashed lines). Used parameters:  $t_c = 20$  fs,  $J(\omega_{\text{vib}}) = 3.5 \times 10^{-4}$ /fs (corresponding to the life-time  $\tau_1 \approx 450$  fs).

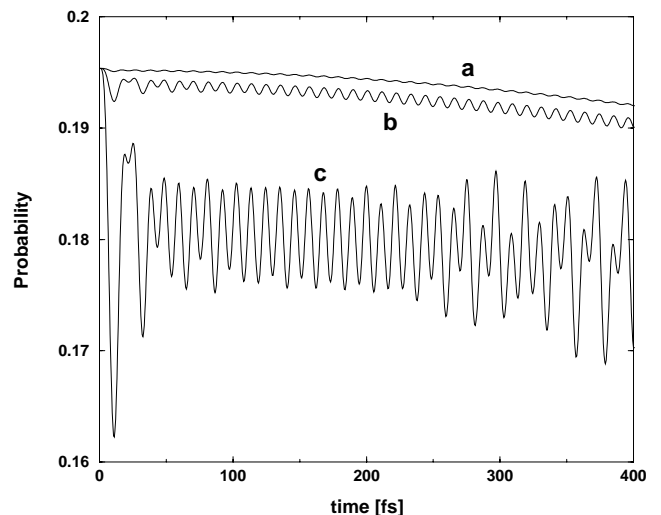


**Fig. 4.** Occupation probability of the fourth excited oscillator level based on the solution of the non-Markovian QME for  $J(\omega_{\text{vib}}) = 3.7 \times 10^{-5}$ /fs (corresponding to the life-time  $\tau_1 \approx 1090$  fs) and (a)  $t_c = 10$  fs, (b)  $t_c = 20$  fs and (c)  $t_c = 30$  fs.

about 400 fs) of the level population from those for smaller  $t_c$ . Furthermore, the solution of the non-Markovian as well Markovian QME results in a same behavior as already discussed in relation to Figure 3.

In order to present the influence of the different choices of the coupling strength  $j_0$  and the correlation times  $t_c$  more clearly, we show in Figures 4 and 5 only the time-development of  $P_4$ . Figure 4 displays the effect of increasing  $t_c$  while keeping the same Markov limit. In the case where the correlation time becomes shorter than the characteristic time of the system (case a) the non-Markovian dynamics are almost identical with the corresponding Markov case. Since we found that all Markovian

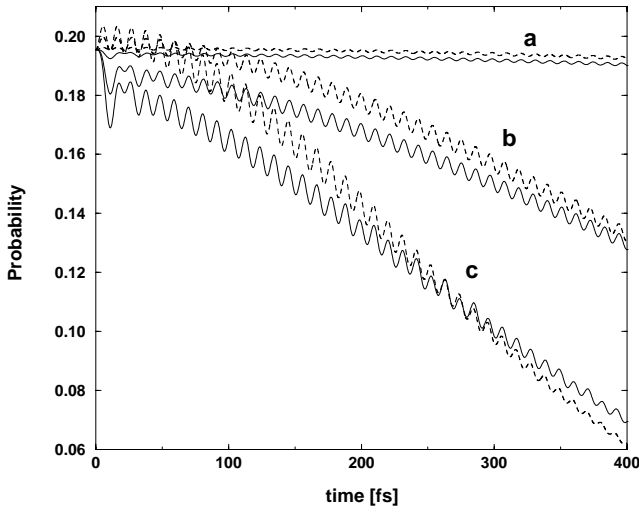


**Fig. 5.** Occupation probability of the fourth excited oscillator level based on the solution of the non-Markovian QME (full line) compared to the solution applying the Markov approximation (dashed-line) for  $t_c = 20$  fs and (a)  $J(\omega_{\text{vib}}) = 3.7 \times 10^{-5}/\text{fs}$  (corresponding to the life-time  $\tau_4 \approx 1090$  fs) (b)  $J(\omega_{\text{vib}}) = 1.9 \times 10^{-4}/\text{fs}$  ( $\tau_4 \approx 210$  fs) (c)  $J(\omega_{\text{vib}}) = 3.5 \times 10^{-4}/\text{fs}$  ( $\tau_4 \approx 110$  fs).

dynamics solutions with different  $t_c$  differ only by the amplitude of the population oscillations, this case also shows in which area of the graph, we would find the solutions of the Markov QME for other values of  $t_c$ . Hence, we can conclude from Figure 4 that an increase of  $t_c$  leads to an increase of the level population oscillations.

On the other hand, Figure 5 presents the influence of an increasing coupling strength  $j_0$  while keeping  $t_c$  constant. As expected the increase of  $j_0$  leads to the steeper decay of the population on the excited levels. Further examination of the time development of the populations shows, that also the deviation between Markov and non-Markov solutions increase with increasing coupling, so that finally, the non-Markov solution cannot be reproduced by the slippage of the initial condition of its Markov limit. In such an attempt, the transition rates would also have to be modified. Finally, it can be stated that differences between the solution of the non-Markovian QME and the QME in the Markov approximation are mainly reduced to a short initial time interval.

However, at this point it is necessary to stress that such a conclusion can be done only with respect to the second order QME which was used to demonstrate the applicability of our method here. The polynomial method itself is independent of the order of the perturbation theory and can be in principle implemented to study the behavior of the system in higher orders of perturbation theory also.

Finally, the motion of the initially prepared wavepacket is shown in Figure 6 where the probability distribution  $P(Q, t)$  has been drawn *versus* the oscillator coordinate and time. Having the density matrix elements  $\rho_{MN}(t)$  at hand it is easy to compute  $P(Q, t)$ . This quantity is directly derived from the coordinate representation of the density operator, *i.e.*  $P(Q, t) = \rho(Q, Q; t)$  in using

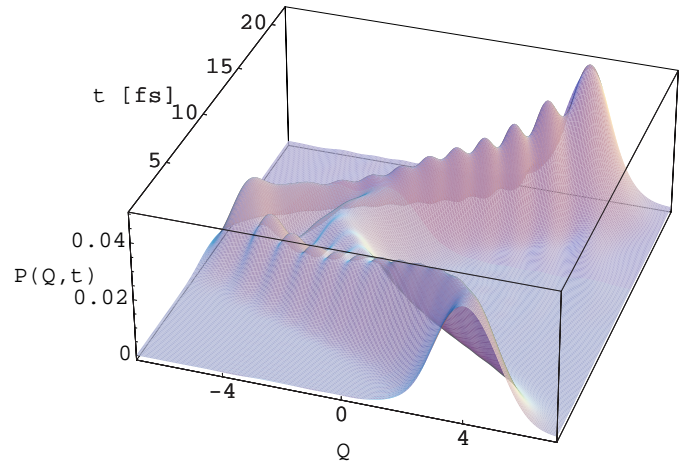


**Fig. 6.** Wavepacket dynamics following from the solution of the non-Markovian QME for  $t_c = 100$  fs and  $J(\omega_{\text{vib}}) = 1.52 \times 10^{-12}/\text{fs}$ .

$\rho(Q, Q; t) = \sum_{M,N} \chi_M(Q) \chi_N^*(Q) \rho_{MN}(t)$ . (The  $\chi_M(Q)$  denote the harmonic oscillator *eigenfunctions*.) In order to display the formation of a double structure in  $P(Q, t)$  the wavepacket motion has been drawn in Figure 6 for the relatively large value  $t_c = 100$  fs. An explanation for the dip in the wavepacket is given in Appendix B *via* an analytical solution of the non-Markovian QME in the limit of a large  $t_c$ . Here, we only state that the obtained behavior of the oscillator wavepacket provides the absence of correlations between the oscillator and the bath at the initial time.

## 5 Conclusions

In the present work we adapted the Laguerre polynomial expansion to solve the non-Markovian QME including in its dissipative part a general form of the correlation function. We tested the accuracy and applicability of the method at a standard model of an open quantum system interacting with a thermodynamic bath. Further we compared our results with those obtained within the Markov approximation. As the main characteristics of non-Markovian dynamics we have to mention here (i) the *slippage* of the early part of the dynamics compared to the Markov case, (ii) the deviations with respect to the long-time behavior, *i.e.* deviations between (effective) relaxation rates, and (iii) the formation of a double structure in the vibrational wavepacket.

The problem of non-physical probabilities obtained for some values of the parameters have been noted and related to the break-down of the perturbation theory. A possible generalization of the Laguerre polynomial method to problems characterized by time-dependent Hamiltonian will be discussed elsewhere [8].

Finally, we comment on some other recently published polynomial expansion methods [31,32]. Firstly, it is necessary to state that they have been exclusively developed to integrate Markovian equations. This is achieved



in using short time propagators constructed with the help of the polynomial expansion of the time-evolution operator. The main difference between our Laguerre polynomial approach and these methods is that the latter provides a step-by-step solution. The Laguerre polynomial method, however, gives the approximation of the density operator in the complete time-interval of interest. This is of course necessary since within non-Markovian dynamics one needs the density matrix not only for the actual time  $t$  but also for earlier times.

The Laguerre polynomials may also give a short-time expansion of a time-evolution operator and thus the solution of a Markovian equation of motion. Certainly, the drawback in such a scheme is that the expansion coefficients involve an inversion of the Liouvillian [23], which has to be held in the computer memory. For large systems this results in a decreasing efficiency since the Liouvillian expanded in a basis of  $N$  functions has  $N^4$  components. This indicates that the power of the Laguerre polynomial method lies in the domain of non-Markovian equations. This will be illustrated in some forthcoming papers.

We gratefully acknowledge financial support by the *Deutsche Forschungsgemeinschaft* through grant Ma 1356/4-2.

## Appendix A: Evaluation of the memory expansion coefficients

In Section 3 we claimed that the integrals (24) can be evaluated analytically. Here we want to give some more details to this statement. The main idea of the following is to divide an integral in some analytically treatable parts. As it is mentioned above the function  $C_{\text{spl}}^{(j)}(t)$  in (24) is an interpolation of the correlation function by cubic splines, *i.e.*

$$C_{\text{spl}}^{(j)}(\theta t_{\text{char}}) = \alpha(\theta)C(\theta_j t_{\text{char}}) + \beta(\theta)C(\theta_{j+1} t_{\text{char}}) + \gamma(\theta)C''(\theta_j t_{\text{char}}) + \delta(\theta)C''(\theta_{j+1} t_{\text{char}}). \quad (28)$$

The four different expansion coefficients can be all expressed by the first one which reads

$$\alpha(\theta) = \frac{\theta_{j+1} - \theta}{\Delta\theta} \equiv \frac{1}{\Delta\theta}(L_1(\theta) - L_1(\theta_{j+1})). \quad (29)$$

Here, we introduced  $\Delta\theta = \theta_{j+1} - \theta_j$ . The remaining three coefficients are

$$\beta(\theta) = 1 - \alpha(\theta), \quad (30)$$

$$\gamma(\theta) = \frac{(\Delta\theta)^2}{6}(\alpha^3(\theta) - \alpha(\theta)), \quad (31)$$

and

$$\delta(\theta) = -\frac{(\Delta\theta)^2}{6}(\alpha^3(\theta) - 3\alpha^2(\theta) + 2\alpha(\theta)). \quad (32)$$

The second derivative  $C''$  of  $C(\theta t_{\text{char}})$  at  $\theta = \theta_j, \theta_{j+1}$  are computed using a standard interpolating algorithm [26]. The above given relations indicate that it is necessary to compute integrals of type equation (24) but with  $C_{\text{spl}}^{(j)}(\theta t_{\text{char}})$  replaced by  $\alpha(\theta)$  up to its third power. In carrying out these integrations it is useful to generate recurrence formulas. Therefore we define

$$a_n^{(m)} = \int_{\theta_j}^{\theta_{j+1}} d\theta (L_1(\theta))^m L_n(\theta) e^{i\Delta\tilde{\omega}\theta} e^{-\theta}. \quad (33)$$

In particular we have  $a_0^{(1)} = a_1^{(0)}$ , and

$$a_0^{(0)} = -\frac{1}{1 - i\Delta\tilde{\omega}} \left[ e^{-(1 - i\Delta\tilde{\omega})\theta} \right]_{\theta_j}^{\theta_{j+1}}, \quad (34)$$

where the abbreviation  $[g(\theta)]_b^a = g(a) - g(b)$  has been introduced. These expression enables us to express the required integrals as

$$\int_{\theta_j}^{\theta_{j+1}} d\theta \alpha(\theta) L_n(\theta) e^{i\Delta\tilde{\omega}\theta} e^{-\theta} = \frac{1}{\Delta\theta} (a_n^{(1)} - a_n^{(0)}), \quad (35)$$

$$\int_{\theta_j}^{\theta_{j+1}} d\theta \alpha^2(\theta) L_n(\theta) e^{i\Delta\tilde{\omega}\theta} e^{-\theta} = \frac{1}{\Delta\theta^2} \left( a_n^{(2)} - 2L_1(\theta_{j+1})a_n^{(1)} + (L_1(\theta_{j+1}))^2 a_n^{(0)} \right), \quad (36)$$

and

$$\int_{\theta_j}^{\theta_{j+1}} d\theta \alpha^3(\theta) L_n(\theta) e^{i\Delta\tilde{\omega}\theta} e^{-\theta} = \frac{1}{\Delta\theta^3} \left( a_n^{(3)} - 3L_1(\theta_{j+1})a_n^{(2)} + 3(L_1(\theta_{j+1}))^2 a_n^{(1)} - (L_1(\theta_{j+1}))^3 a_n^{(0)} \right). \quad (37)$$

Accordingly, the announced recursion formulas which are essential for an efficient computation of  $a_n^m$  read

$$a_n^{(0)} = \frac{1}{1 - i\Delta\tilde{\omega}} \left\{ \left[ e^{i\Delta\tilde{\omega}\theta} e^{-\theta} (L_{n-1}(\theta) - L_n(\theta)) \right]_{\theta_j}^{\theta_{j+1}} - i\Delta\tilde{\omega} a_{n-1}^{(0)} \right\}, \quad (38)$$

and similarly for the other integrals

$$a_n^{(1)} = \frac{1}{1 - i\Delta\tilde{\omega}} \left\{ [L_1(\theta)e^{i\Delta\tilde{\omega}\theta}e^{-\theta}(L_{n-1}(\theta) - L_n(\theta))]_{\theta_j}^{\theta_{j+1}} + a_{n-1}^{(0)} - a_n^{(0)} - i\Delta\tilde{\omega}a_{n-1}^{(1)} \right\}, \quad (39)$$

$$a_0^{(2)} = -\frac{1}{1 - i\Delta\tilde{\omega}} \left\{ [(L_1(\theta))^2e^{i\Delta\tilde{\omega}\theta}e^{-\theta}]_{\theta_j}^{\theta_{j+1}} + 2a_1^{(0)} \right\}, \quad (40)$$

$$a_n^{(2)} = \frac{1}{1 - i\Delta\tilde{\omega}} \times \left\{ [(L_1(\theta))^2e^{i\Delta\tilde{\omega}\theta}e^{-\theta}(L_{n-1}(\theta) - L_n(\theta))]_{\theta_j}^{\theta_{j+1}} + 2a_{n-1}^{(1)} - 2a_n^{(1)} - i\Delta\tilde{\omega}a_{n-1}^{(2)} \right\}, \quad (41)$$

$$a_0^{(3)} = -\frac{1}{1 - i\Delta\tilde{\omega}} \left\{ [(L_1(\theta))^3e^{i\Delta\tilde{\omega}\theta}e^{-\theta}]_{\theta_j}^{\theta_{j+1}} + 3a_0^{(2)} \right\}, \quad (42)$$

and

$$a_n^{(3)} = \frac{1}{1 - i\Delta\tilde{\omega}} \times \left\{ [(L_1(\theta))^3e^{-i\Delta\tilde{\omega}\theta}e^{-\theta}(L_{n-1}(\theta) - L_n(\theta))]_{\theta_j}^{\theta_{j+1}} + 3a_{n-1}^{(2)} - 3a_n^{(2)} - i\Delta\tilde{\omega}a_{n-1}^{(3)} \right\}. \quad (43)$$

At the first glance the given formulas look too complex to be used for the integration of a function of a single variable. But according to the different attempts we undertook to reach sufficient precision they seem to offer the only way to get precise results even for Laguerre polynomials of the order  $10^5$  or higher. Moreover these formulas, if accompanied by a routine to compute Laguerre polynomials *via* standard recurrence formulas [26] can be put in a very compact computer code. Finally, we note that the given spline interpolation scheme to integrate a product of a smooth and a highly oscillating function of type  $\exp i\tilde{\omega}\theta$  may be used in many other cases.

## Appendix B: The limit of a long memory time

This appendix is aimed to demonstrate that an analytical treatment of the non-Markovian QME, equation (4) is possible if the inequalities  $\tau_{\text{mem}} > 1/\omega_{\text{vib}}$  and  $t \gtrsim \tau_{\text{mem}}$  are fulfilled. The first inequality corresponds to the case in which the internal motion of the oscillator (not disturbed by the environment) is faster than the retardation effect resulting from the environmental influence. The second inequality reduces the actual time on the interval from the beginning of the evolution up to times not larger than  $\tau_{\text{mem}}$ . Both inequalities enable us to replace the correlation functions  $C(\tau)$  and  $C^*(\tau)$  by the common and real value  $C(\tau = 0)$ . For the approximative description of the memory effects we write equation (5) as  $\int_0^t d\bar{t} \mathcal{M}(t-\bar{t})\hat{\rho}(\bar{t})$ . Following equation (6) the time-integral can be removed by the definition of a new operator  $\hat{\sigma}$ . It follows the whole QME as

$$\frac{\partial}{\partial t}\hat{\rho}(t) = -\frac{i}{\hbar}[H_S, \hat{\rho}(t)]_- + i[\sqrt{C(0)}K, \hat{\sigma}(t)]_-, \quad (44)$$

with the definition

$$\hat{\sigma}(t) = i \int_0^t d\bar{t} U_S(t-\bar{t}) [\sqrt{C(0)}K, \hat{\rho}(\bar{t})]_- U_S^\dagger(t-\bar{t}). \quad (45)$$

One easily verifies that the equation of motion for  $\hat{\sigma}$  is obtained if we interchange  $\hat{\rho}$  and  $\hat{\sigma}$  in the given equation of motion for  $\hat{\rho}$ . Accordingly one can introduce the new density operators

$$\hat{w}^{(\pm)} = \hat{\rho} \pm \hat{\sigma}, \quad (46)$$

with initial conditions  $\hat{w}^{(\pm)}(t=0) = \hat{\rho}(t=0)$  (note  $\hat{\sigma}(t=0) = 0$ ). The initial value  $\hat{\rho}(t=0)$  which should be used in the following has been already introduced in equation (25). Furthermore, we note  $\hat{\rho}(t) = (\hat{w}^{(+)}(t) + \hat{w}^{(-)}(t))/2$ . Since the operator  $K$  which appears in the equations (44) and (45) has to be identified with the (dimensionless) oscillator coordinate  $Q$  the contribution  $\sqrt{C(0)}Q$  resulting from non-Markovian dissipation can be incorporated into the oscillator Hamiltonian  $H_S$  by defining shifted potential energy functions

$$U^{(\pm)}(Q) = \frac{\hbar\omega_{\text{vib}}}{4}(Q \mp Q_c)^2 - \frac{\hbar C(0)}{\omega_{\text{vib}}}. \quad (47)$$

The origin of the oscillator potential has been displaced to  $Q_c = 2\sqrt{C(0)}/\omega_{\text{vib}}$ .

The Hamiltonian  $H_S^{(\pm)}$  following from the replacement of  $U$  by  $U^{(\pm)}$  define dissipation-less equation of motions for  $\hat{w}^{(\pm)}$  which solution is obtained as

$$\hat{w}^{(\pm)}(t) = \exp\left(-\frac{i}{\hbar}H_S^{(\pm)}t\right) \hat{\rho}(t=0) \exp\left(\frac{i}{\hbar}H_S^{(\pm)}t\right). \quad (48)$$

Since  $\hat{\rho}(t=0)$ , equation (25) describes a pure state, those states both density operators  $\hat{w}^{(\pm)}$  describe at later times remain pure. In contrast,  $\hat{\rho}(t)$  will describe a mixed state. The pure states corresponding to  $\hat{w}^{(\pm)}$  are given by the propagation of the displaced vibrational ground-state  $D^+(g)|0\rangle$  in the displaced oscillator potential  $U^{(\pm)}$ . Changing to the coordinate representation the solution follows as the moving wavepacket (see, *e.g.* [3])

$$\begin{aligned} \psi^{(\pm)}(Q, t) &= \langle Q | \exp\left(-\frac{i}{\hbar}H_S^{(\pm)}t\right) D^+(g) | 0 \rangle \\ &= \chi_0(Q^{(\pm)}(t)) e^{i\varphi^{(\pm)}(t)}. \end{aligned} \quad (49)$$

Here,  $\chi_0(Q)$  denotes the oscillator ground-state wavefunction which reads in the present notation  $(\mu_{\text{vib}}\omega_{\text{vib}}/\pi\hbar)^{1/4} \exp(-Q^2/4)$  (the phase  $\varphi^{(\pm)}(t)$  can be found in [3]). The time-dependent coordinate  $Q^{(\pm)}(t) = Q \mp Q_c + (2g \pm Q_c) \cos(\omega_{\text{vib}}t)$  describes harmonic (but shape invariant) motion of the wavepacket. Again, we state that the non-Markovian dissipative dynamics discussed here is not described by a (coherent) superposition of the two types of wavefunctions  $\psi^{(\pm)}(Q, t)$ . There only appear a superposition of the related pure-state density operators.

We introduce the respective coordinate distribution function as

$$\begin{aligned} P(Q, t) &= \langle Q | \hat{\rho}(t) | Q \rangle = \frac{1}{2} \langle Q | \hat{w}^{(+)}(t) + \hat{w}^{(-)}(t) | Q \rangle \\ &= \chi_0^2(Q^{(+)}(t)) + \chi_0^2(Q^{(-)}(t)) . \end{aligned} \quad (50)$$

It gives the (phase insensitive) superposition of two independent coordinate distribution functions. In contrast to the case of Markovian dissipation where a single wavepacket is moving the given superposition introduces a specific structure into coordinate distribution  $P(Q, t)$ . This can be seen in Figure 6, where the exact solution of the non-Markovian QME is displayed. The mentioned dip in  $P(Q, t)$  disappears if the memory time is reduced.

## References

1. R. Kubo, M. Toda, N. Hashitsume, *Statistical Physics II: Nonequilibrium Statistical Mechanics*, Springer Series in Solid State Sciences, Vol. 31 (Springer, Berlin 1995).
2. D. Zubarev, V. Morozov, G. Röpke, *Statistical Mechanics of Nonequilibrium Processes*, Vols. 1 and 2 (Wiley-VCH, Berlin, 1996).
3. V. May, O. Kühn, *Charge and Energy Transfer Dynamics in Molecular Systems* (Wiley-VCH, Weinheim, 1999).
4. N. Makri, J. Phys. Chem. A **102**, 4414 (1998).
5. S. Chaturvedi, J. Shibata, Z. Physik B **35**, 297 (1979).
6. H.-P. Breuer, B. Kapper, F. Petruccione, Phys. Rev. A **59**, 1633 (1999).
7. G. Gangopadhyay, D.S. Ray, Phys. Rev. A **46**, 1507 (1992).
8. T. Mančal, V. May, J. Chem. Phys. (in press).
9. J.P. Lavoine, A.A. Villaeys, Phys. Rev. Lett. **67**, 2780 (1991).
10. A.A. Villaeys, J.C. Vallet, S.H. Lin, Phys. Rev. A **43**, 5030 (1991).
11. J.R. Brinati, S.S. Mizrahi, G.A. Prata, Phys. Rev. A **50**, 3304 (1994).
12. A. Suárez, R. Silbey, I. Oppenheim, J. Chem. Phys. **97**, 5101 (1992).
13. M.V. Korolkov, G.K. Paramonov, Phys. Rev. A **55**, 589 (1997).
14. Y.J. Yan, Phys. Rev. A **58**, 2721 (1998).
15. P. Gaspard, M. Nagaoka, J. Chem. Phys. **111**, 5676 (1999).
16. Ch. Meier, D.J. Tannor, J. Chem. Phys. **111**, 3365 (1999).
17. D.H. Schirmer, V. May, Chem. Phys. Lett. **297**, 383 (1998).
18. Th. Renger, V. May, Phys. Rev. Lett. **84**, 5228 (2000).
19. A. Imamoglu, Phys. Rev. A **50**, 3650 (1994).
20. L. Skála, O. Břek, Phys. Stat. Sol. B. **114**, K51 (1982).
21. M. Menšík, J. Phys. Cond. Matt. **7**, 7349 (1995).
22. T. Mančal, Czech. J. Phys. **48**, 463 (1998).
23. T. Mančal, J. Bok, L. Skála, J. Phys. A. **31**, 9429 (1998).
24. K. Blum, *Density Matrix Theory and Applications* (Plenum Press, New York, 1981).
25. A.G. Redfield, Adv. Magn. Reson. **1**, 1 (1965).
26. W.H. Press, S.A. Teukolsky, W.T. Vetterling, B.P. Flannery, *Numerical Recipes*, 2nd edn. (Cambridge University Press, Cambridge, 1992).
27. M. Abramovitz, I.A. Stegun, *Handbook of Mathematical Functions* (Dover, New York, 1972).
28. G. Sansone, *Orthogonal functions* (Dover, New York, 1991).
29. D.H. Schirmer, V. May, Chem. Phys. **220**, 1 (1997).
30. P. Gaspard, M. Nagaoka, J. Chem. Phys. **111**, 5668 (1999).
31. W. Huisinga, L. Pesce, R. Kosloff, P. Saalfrank, J. Chem. Phys. **110**, 5538 (1999).
32. H. Guo, R. Chen, J. Chem. Phys. **110**, 6626 (1999).